Modulation of the T-Type Cardiac Ca Channel by Changes in Proton Concentration

J. TYTGAT, B. NILIUS, and E. CARMELIET

From the Laboratory of Physiology, KU Leuven, Campus Gasthuisberg, Onderwijs & Navorsing, B-3000 Leuven, Belgium

ABSTRACT Single-channel measurements and whole-cell experiments with the two suction electrode, voltage clamp technique were used to investigate the effects of external and internal proton concentrations on T-type Ca channels in heart muscle cells of the guinea pig. As in the L-type Ca channel, an increase in the external proton concentration decreases T-type currents, while external alkalinization enlarges the currents. In contrast to the L-type Ca channel, however, a change in the internal proton concentration does not modulate T-type Ca currents. The T-type Ca channel is much more sensitive to variations in pH_o than the L-type Ca channel. By the combination of single-channel and whole-cell experiments we can conclude that the observed changes in macroscopic currents are due to (*a*) changes in the single-channel conductance and in the probability of the T-type Ca channel being open, and (*b*) the titration of the negative surface charges in the neighborhood of the T-type Ca channel with shifts of both the activation and inactivation processes of the channel. The pH_o-induced changes in the maximal conductance (g_{max}) of the T-type Ca channel show an apparent pK_a in the range of 7.1–7.5, while the titration of the negative surface charges near the channel shows an apparent pK_a of 7.1 with a concomitant surface potential of −24.6 mV at 5.4 mM $[Ca]_o$. These pK_a values, less acid than the pK_a values found for the pH_o-induced, L-type Ca channel modulation, might imply a physiological importance of this novel type of channel modulation.

INTRODUCTION

Two different types of Ca channels, the L-type and the T-type, have been described in cardiac tissue in single-channel and whole-cell clamp studies (Bean, 1985; Nilius et al., 1985; Mitra and Morad, 1986; Bonvallet, 1987; Hagiwara et al., 1988). These types of channels have also been found in a large number of other excitable tissues (for a list, see Carbone and Lux, 1984, 1987*a*, *b*, and Fox et al., 1987*a*, *b*). The two

Address reprint requests to Dr. J. Tytgat, Laboratory of Physiology, KU Leuven, Campus Gasthuisberg, B-3000 Leuven, Belgium.

The present address of Dr. Nilius is Julius Bernstein Institute of Physiology, Martin Luther University, 4020 Halle (Saale), GDR.

J. GEN. PHYSIOL. © The Rockefeller University Press · 0022-1295/90/11/0973/18 $2.00
Volume 96 November 1990 973–990

types of channels differ in the voltage range of their activation and inactivation, as well as in the microscopic (single-channel) and macroscopic (whole-cell) gating kinetics (for a review, see Hess, 1988). The sensitivity of both types of channels to Ca agonists and antagonists is quite different (Bean, 1985; Nilius et al., 1985; Mitra and Morad, 1986; Fox et al., 1987*a*; Hagiwara et al., 1988; Tytgat et al., 1988*b*). The L-type current, but not the T-type current, can be increased by β-adrenergic modulation (Bean, 1985; Bonvallet, 1987; Tytgat et al., 1988*a*). As shown by many studies, it is also known that an intracellular or extracellular change in the proton concentration modulates the L-type Ca current (Chesnais et al., 1975; Ohmori and Yoshii, 1977; Kurachi, 1982; Yatani and Goto, 1983; Sato et al., 1985; Iijima et al., 1986; Irisawa and Sato, 1986; Satoh and Seyama, 1986; Kaibara and Kameyama, 1988; Krafte and Kass, 1988).

Until now, no information has been available on pH modulation of T-type Ca channels. In this work we present the first evidence that changes in external but not internal proton concentration modulate T-type Ca channels in heart muscle cells. An increase in the external proton concentration decreases T-type Ca currents, while alkalinization enlarges the currents. The change in activity due to a variation in pH_o is much more pronounced for T-type than for L-type Ca channels. The observed modulation in macroscopic currents is due to (*a*) changes in the single-channel conductance as well as in the probability of the T-type Ca channel being open, and (*b*) the titration of the negative surface charges in the neighborhood of the T-type Ca channel, which shifts the activation and inactivation processes of the channel. The pH_o-induced changes in the maximal conductance (g_{max}) of the T-type Ca channel show an apparent pK_a in the range of 7.1–7.5, while the titration of the negative surface charges near the channel shows an apparent pK_a of 7.1 with a concomitant surface potential of −24.6 mV at 5.4 mM $[Ca]_o$. These pK_a values are less acid than the pK_a values found for the pH_o-induced L-type Ca channel modulation (Satoh and Seyama, 1986; Krafte and Kass, 1988). The pK_a values for the T-type Ca channel might be of much more physiological importance than those for the L-type Ca channel for this novel type of channel modulation.

METHODS

Single guinea pig ventricular myocytes were dissociated by enzymatic dispersion similar to the one described by Mitra and Morad (1985). Experiments were performed at room temperature (20–25°C) using the patch clamp technique (Hamill et al., 1981) in the cell-attached mode for measuring the single-channel currents, and in the whole-cell clamp configuration with two suction pipettes (Axopatch and Axoclamp 2-A amplifier; Axon Instruments, Inc., Foster City, CA). Pipettes were fabricated from borosilicate glass and coated with Sylgard in the case of single-channel experiments (tip resistances of ~1 MΩ). In the whole-cell mode typical pipette resistances ranged from 3 to 6 MΩ. For single-channel analysis we studied pH effects in 51 cells. Whole-cell data were obtained from 45 cells.

Solutions and Current Measurements

Single-channel experiments. In order to zero the membrane potential, the bath solution contained (in mM): 140 K-aspartate, 2 $MgCl_2$, 10 EGTA, 2 ATP, and 10 HEPES titrated with KOH to pH 7.2. The pipette solution contained (in mM): 110 $CaCl_2$ and 10 HEPES or Tris titrated with $Ca(OH)_2$ or HCl to a pH ranging from 6 to 9 according to the performed

experiments. Voltage steps lasting 150 ms were delivered through a pulse generator with a frequency of 1 s^{-1}. The currents were sampled at a rate of 7 kHz using a 12-bit analog-to-digital converter and filtered at 2 kHz with a 4-pole Bessel filter. Each trace contained 1,024 samples. Ensemble average mean currents were normally obtained from 194 traces. The seals in 110 Ca were so stable that no baseline corrections were necessary. The number of channels was estimated from the maximal number of overlapping channel openings in more than 2,000 sweeps. Patches with L-type activity were ruled out based on the different kinetics between L- and T-type Ca channels (bursting behavior, inactivation, mean open times).

Whole-cell experiments. The composition of the internal solution was (in mM): 125 CsCl, 5 MgATP, 15 EGTA, 20 TEA-Cl, and 10 HEPES (pK_a 7.5), buffered with CsOH to pH 6.5, 7.2, or 8 according to the experiments. In some of the experiments 10 HEPES was replaced by 50 HEPES, 10 MOPS (pK_a 7.2), or 5 HEPES in combination with 5 MES (pK_a 6.15) and 5 TAPS (pK_a 8.5). The composition of the external solution was (in mM): 137.6 Tris (pK_a 8.3), 1 $MgCl_2$, 5.4 $CaCl_2$, 5 glucose, and 20 CsCl buffered with HCl/CsOH to a pH ranging from 5.8 to 9. In all experiments K currents were eliminated by using 125 mM CsCl and 20 mM TEA-Cl in the pipette solution and 20 mM CsCl in the bath solution. Na current was eliminated by replacing Na in the bath solution by 137.6 mM Tris (most of the experiments), 137.6 mM MOPS, or a combination of Tris, MES, HEPES, and TAPS, each at a concentration of 34.4 mM. The abolition of the Na current was further checked in some of the experiments with the addition of 30 μM TTX. The L-type Ca current was separated from the T-type Ca current by applying voltage steps (test potentials) from a holding potential of −50 mV where the T-type channel is inactivated (Fox et al., 1987*a*; Hagiwara et al., 1988; Tytgat et al., 1988*a*). The T-type current was separated from the L-type current by applying voltage steps alternatively from holding potentials of −90 and −50 mV. The T-type current was then defined as the difference between the currents from the two holding potentials (Bean, 1985; Hagiwara et al., 1988; Tytgat et al., 1988*a*).

The average total cell capacitance of our cells was 192 ± 17.1 pF (n = 45). Assuming that biological membranes have a specific membrane capacitance of 1 $\mu F/cm^2$, whole-cell Ca currents were expressed as current densities ($\mu A/cm^2$) for comparison between different cells.

The whole-cell currents were sampled at 2 or 5 kHz and filtered using an 8-pole Bessel filter (3 dB at 500 and 1,250 Hz, respectively).

Pooled data are always presented in mean values ± SEM.

Curve-fitting procedures. Data were fitted with theoretical equations as mentioned in the text using a nonlinear chi-square minimalization routine (Bevington, 1969).

RESULTS

External pH and Single-Channel Current of the T-Type Channel

Fig. 1 shows traces of single-channel currents together with the ensemble averaged currents and the amplitude histograms from two different cell-attached patches. The pH in the pipette was buffered at 6 (Fig. 1 *A*) or 9 (Fig. 1 *B*) and depolarizing pulses to −20 mV were applied from a holding potential of −100 mV. It is obvious that the activity of the channel was much larger in the alkaline pH of 9 than in the acid pH of 6. The smaller average current at pH 6 was due to (*a*) a smaller single-channel current (0.36 pA) compared with 0.52 pA in alkaline pH, and (*b*) a marked lower peak open probability at acid pH (almost zero at pH 6, 0.16 at pH 9).

At pH 9 the deviation from the fit to a single Gaussian in the amplitude histogram resulted from a subconductance state seen in some of the sweeps in Fig. 1 *B* (see also Droogmans and Nilius, 1989).

The change in conductance was further analyzed over a broader range of potentials and pH values. Fig. 2 shows an example of the pH-induced changes in the single-channel conductance as a function of potential in two different cells. The amplitude histograms were fitted with two or three Gaussian functions. When fitted with a single Gaussian, a deviation from the fit was present at pH 9 and reflected a subconductance level (see also Fig. 1 *B*). At a pH of 6, mean amplitudes of 0.37 and 0.31 pA were obtained at −40 and −10 mV, respectively (Fig. 2, *A* and *B*). In contrast, at pH 9 mean amplitudes of 0.65 and 0.35 pA were measured at −30 and 0 mV, respectively (Fig. 2, *C* and *D*). From the same cells, all single-channel

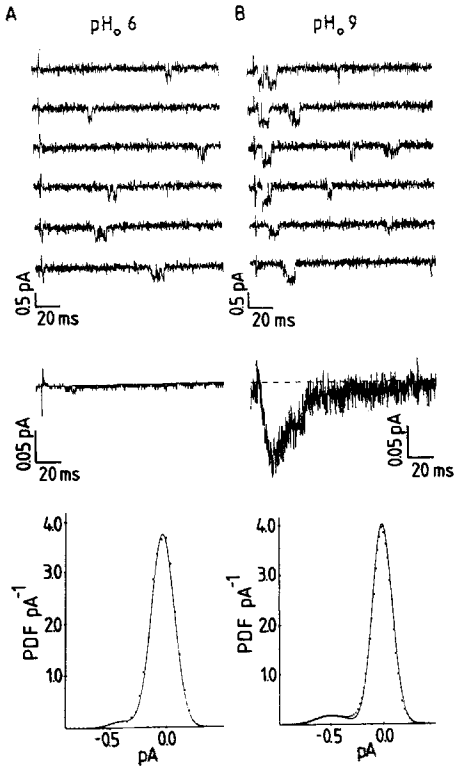

FIGURE 1. Single T-type Ca channel recordings from two different cells at pH 6 (*A*) and pH 9 (*B*). Selected sweeps without nulls are plotted. The ensemble averaged currents are from 194 sweeps (nulls included). From a holding potential of −100 mV, a test potential of −20 mV is applied. The respective amplitude histograms are shown in the lower panel. The amplitude of the single-channel current is calculated from Gaussian fits to 0.36 pA at pH 6 and to 0.52 pA at pH 9. The deviation from the fit to a single Gaussian results from a subconductance state. Null sweeps are not included in the amplitude histograms.

amplitudes of the fully open channel were plotted against the respective voltages (Fig. 2 *E*). From linear fits, single-channel conductances of 3.5 and 10.8 pS were obtained for pH 6 and 9, respectively.

Fig. 3 presents pooled data from the 51 cells studied for the single-channel conductance as a function of pH, and shows that acidification reduces the single-channel conductance, whereas alkalinization has the opposite effect.

As evident from Fig. 1, pH not only changed the single-channel conductance, but also the open probability. In the following set of experiments, a more detailed analysis was made of the open probability as a function of potential and pH.

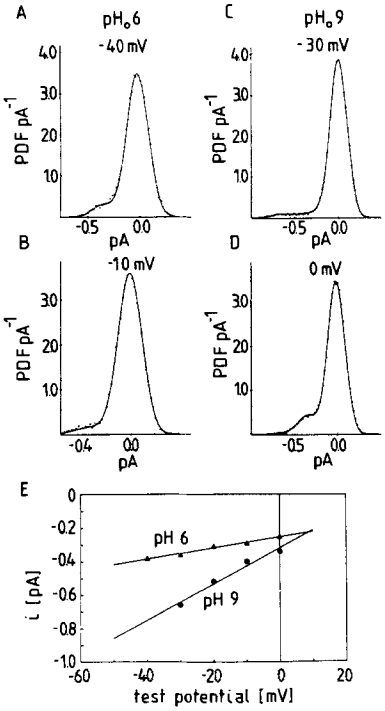

FIGURE 2. *I-V* relationships for unitary T-type Ca currents at two different pH values from two individual cells. *A–D* show amplitude histograms at two different voltages for two pH values (−40 and −10 mV for pH 6, −30 and 0 mV for pH 9). The *I-V* plot in *E* is constructed from all data of the same cells. From linear fits a slope conductance of 3.5 pS at pH 6 and 10.8 pS at pH 9 is calculated with the respective regression coefficients of 0.98 and 0.97.

Fig. 4, *A* and *B* shows average currents from cell-attached patches obtained under different experimental conditions. The currents were fitted with the equation

$$I = a_1 * [1 - \exp(-t/\tau_m)]^2 * \exp(-t/\tau_h), \quad (1)$$

where τ_m and τ_h represent the activation and inactivation time constants. Peak open probabilities were then calculated using the equation

$$I_{peak} = N * i * P_{peak}, \quad (2)$$

where I_{peak} is the peak current, N the respective number of channels, i the single-channel current, and P_{peak} the peak value of probability of the channel being open. At a pH of 8.5 (Fig. 4 *B*) the P_{peak} values exceeded those at pH 6.5 (Fig. 4 *A*).

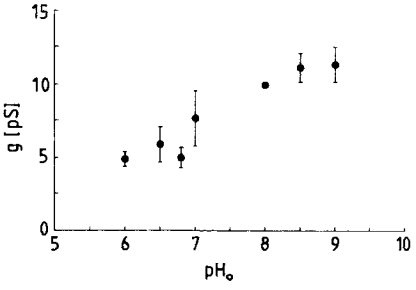

FIGURE 3. pH dependence of the single-channel conductance (*g*). Acidification reduces *g*, whereas alkalinization shows the opposite effect. The data are obtained from 51 cells.

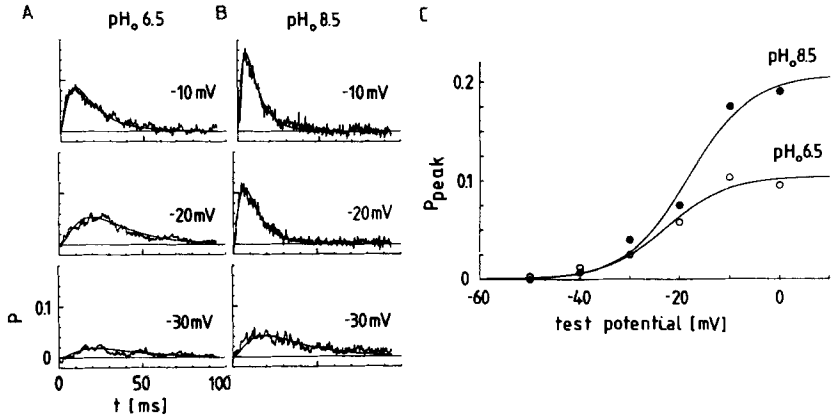

FIGURE 4. Voltage and time dependence of the probability of the T-type Ca channel being open at two different pH values as measured from the ensemble averaged currents of two different cells. From a holding potential of −120 mV, different test potentials are applied. The currents in the six panels on the left (*A* and *B*) are fitted with Eq. 1, and peak open probabilities (*P*) are calculated using Eq. 2. At pH 6.5 and from −10 to −30 mV, a ranged from 0.23 to 0.08, τ_m from 4.8 to 15.4 ms, and τ_h from 14 to 24 ms. At pH 8.5 and from −10 to −30 mV, a ranged from 0.39 to 0.14, τ_m from 2.6 to 11.3 ms, and τ_h from 8.3 to 24.1 ms. The voltage dependence of the peak probability of the channel being open as obtained from similar fits from two other cells is shown in *C*. The smooth lines are obtained from best fits using Eq. 3, where at pH 6.5 $P_{max} = 0.1$, $V_{1/2} = -22$ mV, and $s = 6.2$ mV, and at pH 8.5 $P_{max} = 0.2$, $V_{1/2} = -18.3$ mV, and $s = 6.25$ mV. The used averaged currents are obtained from 194 sweeps each. Data points are sampled with 150-μs intervals and filtered with 2 kHz.

Values of P_{peak} for two other cells over a broader range of potentials are plotted in Fig. 4 *C*. The data were fitted by a Boltzmann equation

$$P_{peak} = P_{peak,max}/[1 + \exp[-(V - V_{1/2})/s]], \quad (3)$$

where P_{peak} is the peak probability, $P_{peak,max}$ the maximal peak probability of the channel being open, V the test potential, $V_{1/2}$ the potential of half-maximal activation, and s the slope parameter. The data clearly show that the maximum value for the open probability was increased in alkaline pH (from 0.1 at pH$_o$ 6.5 to 0.2 at pH$_o$ 8.5). The potential for the half-maximal value, $V_{1/2}$, was −18.3 mV for pH$_o$ 8.5 and −22 mV for pH$_o$ 6.5. Pooled data for $V_{1/2}$ as a function of pH from the 51 cells studied are given in Fig. 5, and confirm that no significant voltage shift exists for the

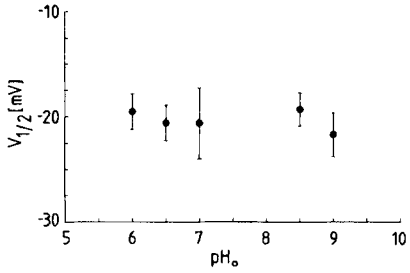

FIGURE 5. pH dependence of the potential of half-maximal activation ($V_{1/2}$). Pooled data from all 51 cells studied are shown. No significant correlation between pH and $V_{1/2}$ in the presence of 110 mM [Ca] can be obtained.

activation process. The absence of a voltage shift is not unexpected since the results were obtained in 110 mM [Ca], a concentration of divalent ions probably more than sufficient to saturate negative fixed charges. Consistent with this result, time constants for activation (τ_m) did not change with pH: at a test potential of −20 mV τ_m was 4.9 ± 0.6 ms (pH 6 and 6.5, $n = 16$), 6.0 ± 0.7 ms (pH 7, $n = 7$), and 6.5 ± 1.1 ms (pH 8.5 and 9, $n = 22$). These changes were not significant. A similar observation was made for the time constants of inactivation (τ_h). At −20 mV τ_h was 19.7 ± 1.8 ms at pH 8.5 and 9 ($n = 22$), while acidification to pH 6.5 showed a τ_h of 21.1 ± 2.1 ms ($n = 7$).

In accord with these findings, other kinetic parameters such as short and long mean closed time (τ_{c1}, τ_{c2}), mean open time (τ_o), average first latency (t_L), and average open and closed times (t_o, t_{cl}) did not vary for changes in pH between 6 and 9.

Fig. 4 clearly showed that the maximum value of open probability, i.e., the saturating value of the Boltzmann distribution obtained at ~0 mV, was dependent on pH. Fig. 6 summarizes the data of all 51 experiments with P_{max} as a function of pH. It can be seen that acidification reduces P_{max}, whereas alkalinization shows the opposite effect. The changes in P_{max} were not caused by pH_o-induced changes in τ_{c1},

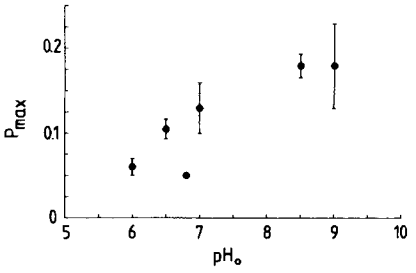

FIGURE 6. pH dependence of the maximal probability of the channel being open (P_{max}). Acidification reduces P_{max}, whereas alkalinization shows the opposite effect. The data are obtained from 51 cells.

τ_{c2}, τ_o, t_L, t_o or t_{cl}. In contrast, this dependence mainly reflected a change in the probability of observing sweeps without openings (nulls). The apparent probability of observing a null (P_A) was calculated by

$$P_A = P_{AN}(O)^{1/N}, \tag{4}$$

where N is the number of channels in the patch as obtained from the maximal number of overlapping events from usually >2,000 sweeps, and $P_{AN}(O)$ the number of observed nulls divided by the number of sweeps. At a test potential of −20 mV, P_A was changed from 0.59 ± 0.04 ($n = 12$) at pH 9 and pH 8.5 to 0.83 ± 0.03 at pH 6.5 ($n = 9$). From the same material, a P_A value at pH 7 of 0.65 ± 0.02 ($n = 26$) has been reported by Droogmans and Nilius (1989).

By combining the information in Figs. 3 and 6, the maximal conductance, g_{max} (complete activation), can be calculated. The dependence of g_{max} on external pH is plotted in Fig. 7. The best fit was obtained using the equation

$$g_{max} = [a/[1 + (K_d/c)^h]] + b, \tag{5}$$

where $a = 1.92$ pS, $b = 0.14$ pS, $K_d = 0.08$ μM, and $h = -1$. The K_d value

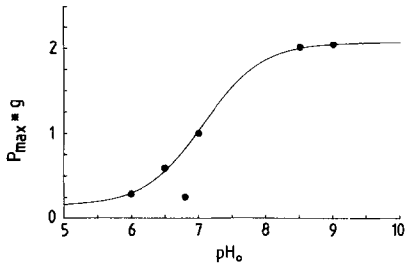

FIGURE 7. pH dependence of the maximal conductance ($g_{max} = P_{max} * g$). The smooth curve through the data obtained from Figs. 3 and 6 is fitted using Eq. 5, where $a = 1.92$ pS, $b = 0.14$ pS, $K_d = 0.08$ μM, and $h = -1$. From the fit of $P_{max} * g$ as a function of pH, a pK_a value of 7.1 is obtained.

corresponds to a pK_a value of 7.1 (g_{max} at pH 6.8 was ignored for the fit, since it appeared to be way out of the range of all other experimental points).

External pH and Whole-Cell Current of the T-Type Channel

Experiments similar to those with cell-attached patches were repeated in the whole-cell configuration. These experiments did not require the use of elevated [Ca] and allowed an analysis of the channel behavior under more physiological conditions.

The whole-cell current traces in Fig. 8 show that external changes in pH modify T-type Ca currents in the same manner as for the cell-attached patches. T-type currents in Fig. 8 are determined as described in the methods: i.e., by calculating the difference between the currents evoked from -90 and -50 mV (V_{hold}) to -30 mV (V_{test}). External acidification to a pH of 6.8 (Fig. 8 *A*) reduced the T-type current with respect to the current at pH 7.4 (Fig. 8 *B*). In contrast, alkalinization to a pH of 7.7 increased the T-type Ca current (Fig. 8 *C*). Upon alkalinization, the rate of activation became faster, whereas the rate of inactivation was not affected.

The same type of experiments were repeated but the test potential was varied over a range of -50 to $+20$ mV. Examples for test potentials of -50, -40, and -30 mV

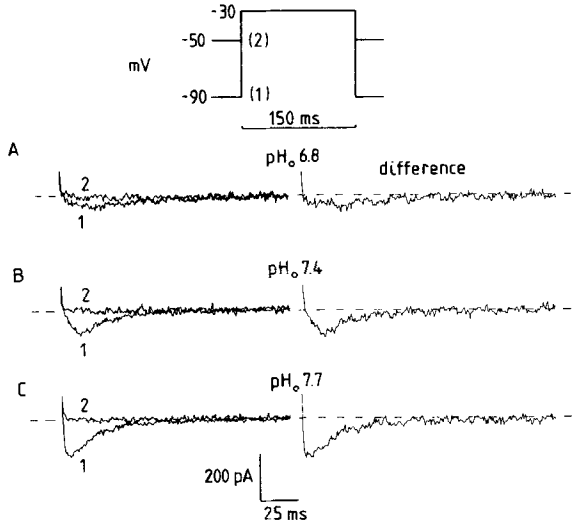

FIGURE 8. External changes in pH modulate whole-cell recorded $I_{Ca,T}$. As described in the methods, $I_{Ca,T}$ is defined as the difference current evoked from V_{hold} -90 mV (*1*) and V_{hold} -50 mV (*2*) to V_{test} -30 mV. As can be seen from the traces of the same cell, external acidification from pH 7.4 (*B*) to pH 6.8 (*A*) reduces $I_{Ca,T}$. Alkalinization to pH 7.7 (*C*) enhances $I_{Ca,T}$ amplitude.

at external pH values of 6.5, 7.4, and 8 are given in Fig. 9 *A*, *B*, and *C*, respectively. Peak currents pooled from 5–14 cells are given as an *I-V* relationship in Fig. 9 *D*. By the use of standardized whole-cell currents (see Methods) we were able to compare different cells tested under different conditions. Smooth curves through the symbols in Fig. 9 *D* were fitted using the formula

$$I = g_{max} * (V - V_{rev})/[1 + \exp[-(V - V_{1/2})/s]], \quad (6)$$

where g_{max} = maximal conductance in mS/cm^2, V = test potential in mV, V_{rev} = extrapolated reversal potential in mV, $V_{1/2}$ = potential of half-maximal activation in mV, and s = slope parameter in mV.

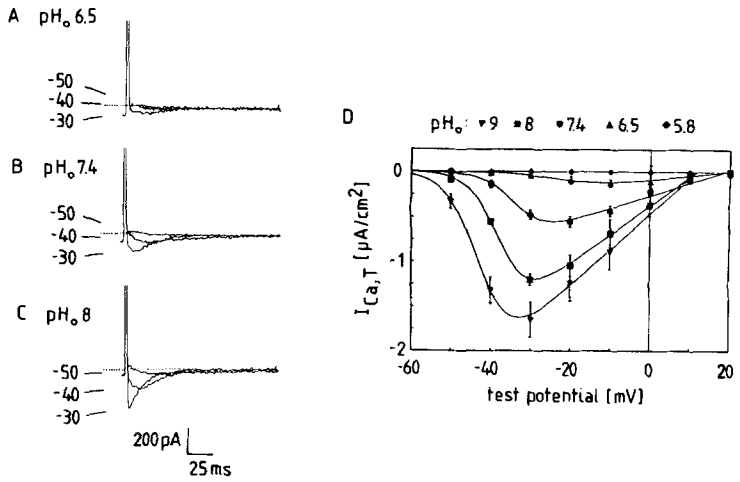

FIGURE 9. Voltage dependence of $I_{Ca,T}$ as a function of pH$_o$. *A–C* show difference currents from the same cell at three different pH$_o$'s: 6.5 (*A*), 7.4 (*B*), and 8 (*C*). V_{test} was −50 mV, −40 mV, and −30 mV, respectively. The increase in external protons (pH 7.4 to 6.5) strongly reduces $I_{Ca,T}$, while a decrease (pH 7.4 to 8) shows the opposite effect. *D* summarizes the peak difference currents at different V_{test} as a function of pH$_o$. The currents are standardized as μA/cm^2 and are obtained from different cells. Each point represents at least 5 and at most 14 cells. Smooth curves through the symbols are fitted using Eq. 6. It is clear that peak amplitude at pH 7.4 is reduced by 75 and 100% upon acidification to pH 6.5 and 5.8, respectively. In contrast, it is enlarged two- and even threefold upon alkalinization to pH 8 and 9, respectively. External changes in pH also cause a shift of the peak of the *I-V* relationship: 14 mV between pH 7.4 and 6.5, 5 mV between pH 7.4 and 8, and 11 mV between pH 7.4 and 9.

The advantage of using Eq. 6 is that the fits provide information about pH$_o$-induced changes in g_{max} and V_{rev}, as well as in the activation process ($V_{1/2}$ and s) of the channel. However, two limitations have to be kept in mind when using Eq. 6: (*a*) only the linear part of the *I-V* relationship gives a fair g_{max} value, and (*b*) E_{rev} is derived by linear extrapolation and does not take into account an eventual rectification close to the true reversal potential. Raising pH$_o$ from 6.5 to 7.4, 8, and finally 9 induced the following changes: (*a*) g_{max} increased from 0.004 to 0.014, 0.032, and 0.039 mS/cm^2, (*b*) V_{rev} shifted from 19 to 18.7, 11.7, and 11.7 mV; (*c*) $V_{1/2}$ shifted

from −21 to −33, −37, and −41 mV; and (*d*) s changed from 5.9 to 3.9, 3.7, and 3.9 mV. As can be seen from Fig. 9 *D*, the peak of the *I-V* relationship was increased with a factor of 2 and 3 for pH_o changes from 7.4 to 8 and 9, respectively. Acidification from pH 7.4 to 6.5 reduced the peak by 75%, and stronger acidification to pH 5.8 abolished the T-type current completely.

A plot of g_{max} as a function of pH_o (over the broad range of pH_o 4–9) is presented in Fig. 10. The graph also includes a comparison with the same parameters for the L-type channel obtained in the same cells using identical solutions ($n = 8$). Smooth

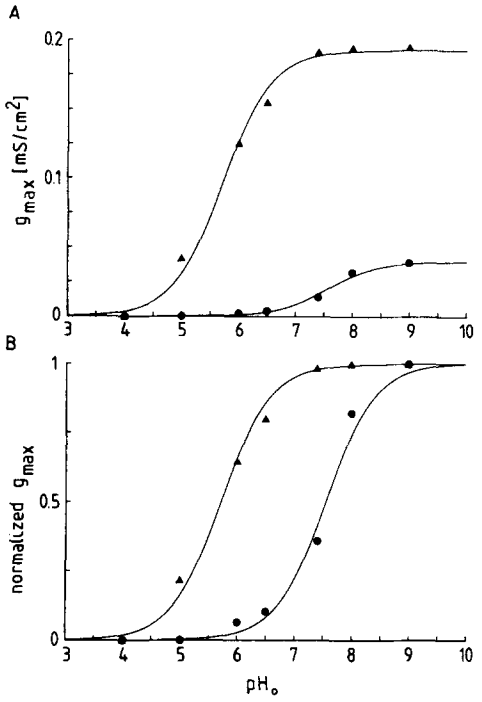

FIGURE 10. pH_o dependence of g_{max} for the T-(*circles*) and L-type (*triangles*) Ca channel. *A*, The values of g_{max} are obtained using Eq. 6 and ranged for the L-type Ca channel from 0 to 0.195 mS/cm^2 from pH_o 4 to 9, and for the T-type Ca channel from 0 to 0.039 mS/cm^2 from pH_o 4 to 9. The fit through the symbols is obtained using Eq. 7, where for the T-type Ca channel a = 0.039 mS/cm^2, K_d = 0.03 μM, and $h = -1$, and for the L-type Ca channel a = 0.196 mS/cm^2, K_d = 1.91 μM, and $h = -1$. The K_d values indicate a pK_a of 7.52 and 5.72 for the T- and L-type Ca channels, respectively. Taking into account the acid pK_a value for the L-type channel (5.72), the pK_a value of 7.52 for the T-type obtained with the whole-cell experiments fairly approximates the pK_a of 7.1 obtained from the single-channel results (see Fig. 7). *B*, Normalized g_{max} for the T-type and L-type Ca channel as a function of pH_o.

curves were fitted using the formula

$$g_{max} = a/[1 + (K_d/c)^h], \tag{7}$$

where a is the maximal conductance, c the proton concentration, and h the cooperativity parameter. In Fig. 10 *A* the results are given in absolute values and emphasize the much larger g_{max} value for the L- compared with the T-type channel. For the L- and T-type channels, the maximal effect (a) was 0.196 and 0.039 mS/cm^2, respectively. The K_d for the L- and T-type channels was 1.91 and 0.03 μM, which corresponds to a pK_a of 5.72 and 7.52, respectively. The parameter h was equal to −1. Fig. 10 *B* shows normalized g_{max} as a function of pH_o. This representation clearly emphasizes that small changes around the physiological pH_o of 7.4 influence much stronger g_{max} in T-type than in L-type Ca channels.

Channel Gating

In Fig. 9 *D*, not only the peak but also the potential at which the peak occurred were shifted as a function of the external pH. At pH 7.4 the peak of the *I-V* relationship was situated near −23 mV, while acidification to pH 6.5 caused a 14-mV shift of the peak to −9 mV. In contrast, 5- and 11-mV shifts of the peak to −28 mV and −34 mV were seen by external alkalinization from pH 7.4 to pH 8 and 9, respectively.

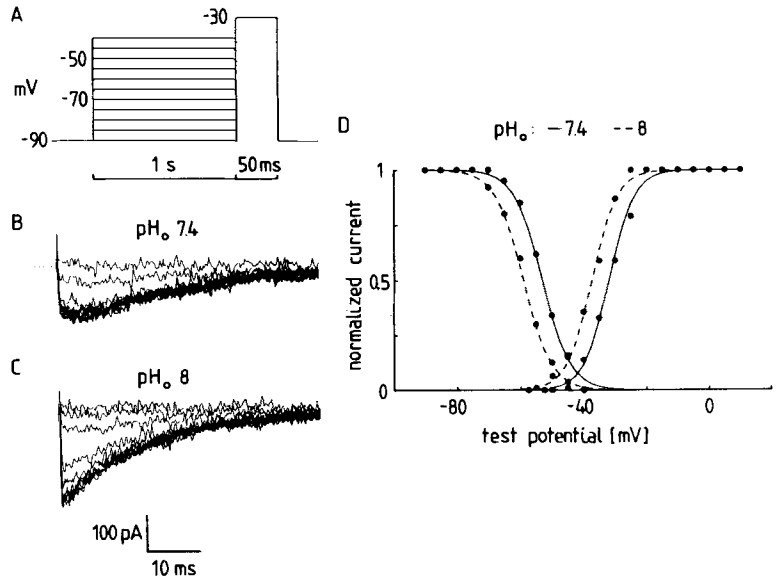

FIGURE 11. pH-induced shifts in T-type Ca channel gating. *A* shows the voltage protocol by which currents are evoked during a 50-ms test pulse at −30 mV immediately after a 1-s prepulse at different potentials. This inactivation voltage protocol is performed at two different proton concentrations: pH 7.4 (*B*) and pH 8 (*C*). *D* summarizes the influence of different proton concentrations on the activation and inactivation curves. The data for the activation and inactivation curves are fitted to the Boltzmann equation (Eq. 3) $I/I_{max} = 1/[1 + \exp[\pm(V\text{-}V_{1/2})/s]]$, where I/I_{max} is the normalized peak inward current evoked during the test pulse, V the test potential, $V_{1/2}$ the voltage for half-maximal (in-)activation ($V_{1/2}$ inactivation: −59 mV and −54 mV for pH 8 and 7.4, respectively), and s the slope parameter (s inactivation: 4.4 mV for pH 8 and 7.4, respectively). Data for the activation curve are taken from Fig. 9 *D*. Activation and inactivation curves are equally shifted to more positive potentials upon increasing the external proton concentration (~5 mV shift for pH 8 to 7.4).

Such a shift suggests changes in the gating of the channel. These aspects will be analyzed in more detail in the next section.

Information from the fit in Fig. 9 *D* was used to construct the activation curve in Fig. 11 *D*. It is clear that the activation curve is shifted to more negative potentials by alkalinization. For the whole range of pH values, the following results were obtained: lowering the pH from 9 to 8 or from 8 to 7.4 caused a shift of 4 mV toward negative potentials without a change in the slope parameter, while lowering the pH from 7.4

to 6.5 induced a much bigger shift of 12 mV toward positive potentials with only a 2-mV change of the slope parameter (see also Fig. 12).

Eventual shifts of the inactivation curve were studied using a two-pulse protocol (Fig. 11 *A*). Holding potential was −90 mV and prepulses (lasting 1 s) varied from −90 to −40 mV. A 50-ms test pulse immediately after the prepulses was set at −30 mV. Changing the external pH from 7.4 to 8 (Fig. 11, *B* and *C*) caused a shift of 4–5 mV in the negative direction without changing the slope parameter (s = 4.4 mV; Fig. 11 *D*). The smooth curves of Fig. 11 *D* were fitted with a Boltzmann equation similar to Eq. 3.

A plot of $V_{1/2}$, i.e., the potential at which activation or inactivation is half-maximal, as a function of pH_o is given in Fig. 12. The $V_{1/2}$ value for pH 7.4 was taken as a reference. The smooth curve through the symbols was fitted using the formula

$$V_{1/2} = a - [b/[1 + (K_d/c)^h]], \tag{8}$$

where a is the potential at which the negative surface charges of the membrane are

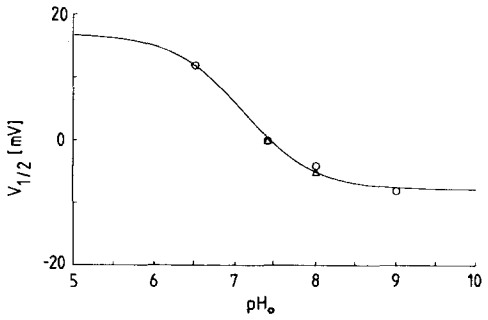

FIGURE 12. Relationship between $V_{1/2}$ and pH_o. Shifts in $V_{1/2}$ value for activation (*circles*) and inactivation (*triangles*) are plotted vs. pH_o. The $V_{1/2}$ value for activation at pH 7.4 is taken as a reference. $V_{1/2}$ values for activation and inactivation are obtained, respectively, from the fits in Fig. 9 *D* using Eq. 6 and from the fits in Fig. 11 *D* using a formula similar to Eq. 3. The fit through the symbols is obtained using Eq. 8, where $V_{1/2} = a-[b/[1 + (K_d/c)^h]]$, where a = −7.7 mV, b = −24.6 mV, K_d = 0.079 μM, and h = 1. The K_d values of 0.079 indicates a pK_a of 7.1.

not neutralized, b the pH_o-sensitive surface potential, c the concentration, and h the cooperativity parameter. We found a K_d value of 0.079 μM, which corresponds to a pK_a of 7.1. The pH_o-sensitive surface potential was −24.6 mV (*b*). The curve was fitted with a value of 1 for h.

T-Type Current Amplitude Is Not Modulated by Internal Changes in pH

Irisawa and Sato (1986) found that changes in external pH could result in changes in pH_i if the buffering capacity of the pipette (intracellular) solution was low. They also showed that the L-type Ca channel was very sensitive to pH_i changes. In order to exclude the possibility that our results with changes in pH_o were due to proton effects at the intracellular side, a number of control experiments were performed. First, the buffer capacity was increased from 10 to 50 mM HEPES in the pipette solution in five whole-cell experiments. These experiments revealed that the extent of the pH_o-modulated T-type currents was not different with respect to the experiments with the normal 10 mM HEPES in the pipette solution. With 50 mM

HEPES in the pipette solution, the following current densities were obtained for a test potential of −30 mV: −0.42 ± 0.06 $\mu A/cm^2$ at pH_o 7.4 ($n = 5$), −1.36 ± 0.18 $\mu A/cm^2$ at pH_o 8 ($n = 3$), and −1.48 ± 0.06 $\mu A/cm^2$ at pH_o 9 ($n = 2$). With 10 mM HEPES in the pipette solution, current densities for a test potential of −30 mV (see also Fig. 9 *D*) were: −0.48 ± 0.05 $\mu A/cm^2$ at pH_o 7.4 ($n = 14$), −1.22 ± 0.06 $\mu A/cm^2$ at pH_o 8 ($n = 8$), and −1.6 ± 0.18 $\mu A/cm^2$ at pH_o 9 ($n = 8$). These pH_o-induced changes were clearly not dependent on the buffer capacity (10 or 50 mM HEPES) in the pipette solution.

Second, we investigated the effect of different pH_i on the T-type current in the whole-cell experiments. We studied 6 cells with 10 mM HEPES inside buffered pH 6.5 or 8 instead of 7.2. Outside, we applied on these cells a broad pH range from 6.5 to 9. With a pipette pH of 6.5, the following results were obtained for a test potential of −30 mV: −0.12 ± 0.06 $\mu A/cm^2$ at pH_o 6.5 ($n = 4$), −0.39 ± 0.08 $\mu A/cm^2$ at pH_o 7.4 ($n = 4$), and −1.26 ± 0.13 $\mu A/cm^2$ at pH_o 8 ($n = 4$). With a pipette pH of 8, the current densities for the same test potential of −30 mV were: −0.06 ± 0.01 $\mu A/cm^2$ at pH_o 6.5 ($n = 2$), −0.31 ± 0.12 $\mu A/cm^2$ at pH_o 7.4 ($n = 2$), and −1.55 ± 0.57 $\mu A/cm^2$ at pH_o 9 ($n = 2$). With the normal pipette pH of 7.2, current densities for a test potential of −30 mV (see also Fig. 9 *D*) were: −0.06 ± 0.02 $\mu A/cm^2$ at pH_o 6.5 ($n = 10$), −0.48 ± 0.05 $\mu A/cm^2$ at pH_o 7.4 ($n = 14$), −1.22 ± 0.06 $\mu A/cm^2$ at pH_o 8 ($n = 8$), and −1.6 ± 0.18 $\mu A/cm^2$ at pH_o 9 ($n = 8$). In summary, pH_o-induced changes in T-type current densities were not dependent on the pH of the pipette (=pH_i) between pH_i 6.5 and 8.

It can further be stressed that all the experiments were performed in Na-free conditions. This eliminates any secondary change of pH_i due to activity of the Na-H exchange mechanism (Irisawa and Sato, 1986). Consistent with the above-mentioned observations, single-channel activity in the cell-attached configuration did not change upon varying the pH values in the bath solution between 6 and 9.

Does HEPES or Tris Itself Interact with L- and T-Type Ca Channels?

To exclude a possible effect of the HEPES or Tris buffer itself on the L- and T-type Ca channel, two other control experiments were performed in the whole-cell mode. First, two cells were clamped with MOPS as internal and external buffer. Inside the pH was set at 7.2 and outside we changed the pH from 6.5 to 8. Here, too, identical T-type Ca current densities were noticed with respect to the use of the HEPES and Tris buffer. Second, experiments were performed under conditions of having a mixture of four buffers (Tris, HEPES, MES, and TAPS) externally and three buffers (HEPES, MES, and TAPS) internally. The following current densities were obtained for a test potential of −30 mV: −0.21 ± 0.07 $\mu A/cm^2$ at pH_o 6.5 ($n = 3$), −0.61 ± 0.04 $\mu A/cm^2$ at pH_o 7.4 ($n = 4$), and −1.15 ± 0.18 $\mu A/cm^2$ at pH_o 8 ($n = 6$). Compared with the current densities for the same test potential of −30 mV in the presence of 10 mM HEPES buffered at pH 7.2 (see above and Fig. 9 *D*), these changes were not significant.

DISCUSSION

The present experiments have revealed that the T-type Ca channel is modulated by changes in pH_o. Evidence for this modulation is given by pH_o-induced changes in

(*a*) single-channel conductance (*g*), (*b*) open probability (*P*), and (*c*) voltage-dependent gating ($V_{1/2}$).

pH_o-induced Changes in Single-Channel Conductance

pH_o-induced changes in single-channel conductance can be mediated by proton binding in the channel pathway or by protonation of an external binding site. Evidence for the first mechanism has been given by Begenisich and Danko (1983), who found that the voltage dependence of the external proton block was nonmonotonic for the Na channel: depolarized potentials prevented binding of protons within the pore, and negative potentials allowed protons to flow through the pore. Evidence for the external proton binding site mechanism has been given by Prod'hom et al. (1987) for the L-type Ca channel. These authors showed that the on and off rates of H^+ and D^+ ions were independent of the membrane potential, and hence that the protonation binding site was outside the part of the channel which experiences the transmembrane electric field. Moreover, Pietrobon et al. (1988) have shown for the L-type Ca channel that the protonation site is far enough from the permeation pathway so that an entering ion does not experience the different local potential associated with the protonated or unprotonated site. Thus, the different conductances of the L-type channel cannot be explained by a protonation-dependent surface potential at the channel entrance which changes the local concentration of permeant ions. An interesting difference in single-channel conductance between L- and T-type Ca channels is that changes in pH_o alter the single-channel conductance of the T-type channel even in the presence of a divalent cation in the pipette solution (110 [Ca]), whereas the single-channel conductance of the L-type channel is only affected when monovalent ions are used in the pipette solution (Prod'hom et al., 1987; Pietrobon et al., 1988). These authors suggest that a high concentration of divalents in the pipette solution almost saturates the L-type channel occupancy. As a consequence, the channel would always reside in the deprotonated state and hence behave in its highest conductive state, irrespective from the pH_o (between pH 6 and 9). This is clearly not true for the T-type Ca channel.

pH_o-induced Changes in Open Probability

The observed changes in open probability could mean that a change in pH_o sensitively affects a rate coefficient between a closed and an absorbing state, reflecting a change in the probability of observing blank sweeps. The presence of blank sweeps could be interpreted as hibernating channels which will now and then show activity by a modal gating mechanism.

pH_o-induced Changes in g_{max}

By the combination of single-channel conductance and open probability, the observed changes in g_{max} in the whole-cell experiments can also be explained. These changes in g_{max} ($=g * P_{max}$) show an apparent pK_a value in the range of 7.1–7.5 for the T-type Ca channel when they are fitted as a function of pH_o. In contrast, we find a more acid apparent pK_a around 5.72 for the L-type Ca channel of the same cells under the same ionic conditions. This means that upon slightly changing the

extracellular pH away from a normal physiological pH, as for instance in acidosis, the T-type channel will be modulated much stronger than the L-type. This can easily be seen in Fig. 10 *B*. Interestingly, Satoh and Seyama (1986) found that the relative slope conductance of the L-type Ca channel in rabbit sino-atrial node cells could be titrated with a pK_a of 6.4. In addition, our whole-cell experiments provide evidence that the g_{max} of the T-type channel is much more sensitive than the g_{max} of the L-type channel upon equal variations in pH_o. Fig. 10 *A* clearly demonstrates that $g_{max,T\text{-}type}$ is totally abolished at pH_o 5.8 and increased by a factor of 10 for a pH_o change from 6.5 to 9. In contrast, the $g_{max,L\text{-}type}$ is abolished at a pH_o of 4 and increased only by a factor of 1.18 for a pH_o change from 6.5 to 9. Krafte and Kass (1988) have shown, in a relationship between pH_o and peak $I_{Ca,L}$, that the L-type Ca channel is completely blocked at a pH_o of 4.5 and can be increased by a factor of about 1.5 to pH_o 10. Our results nicely confirm their observations for the L-type Ca channel. The kind of amino acid with a pK_a in the range of 7.1–7.5 in the T-type channel protein is involved in the pH_o modulation remains unclear. Histidine is the amino acid with a pK_a most close (pK_a 6.5). However, it must be mentioned that the charges of a protein in the neighborhood of an amino acid will modify the pK_a value of that amino acid. Hence, it is speculative to correlate the experimental observed pK_a value of 7.4 with the pK_a value of any amino acid.

pH_o-induced Gating Shifts

An additional observation in our whole-cell experiments were the pH_o-induced gating shifts. As can be seen in Fig. 5, pH_o-induced changes in gating are absent in our single-channel experiments using 110 mM [Ca] in the pipette solution. In whole-cell experiments, however, pH_o-induced changes in the negative surface charges are sensed by the gates of the T-type channel. The charges can be titrated with an apparent pK_a value of 7.1 with a concomitant surface potential of −24.6 mV at 5.4 mM $[Ca]_o$ in the extracellular solution. Krafte and Kass (1988) concluded that the shifts in channel gating (pK_a 5.8), as induced by changes in pH_o, could not explain all the observations on modulation of the L-type current amplitude. They suggested that an additional mechanism contributed to the modulation and their likely explanation was a proton ion block of the pore. In our study we combined single-channel and whole-cell experiments and could elaborate this additional mechanism. Since (*a*) pH_o-induced gating shifts were absent in our single-channel experiments, and (*b*) there was a high correlation between pH_o-induced changes in $g * P_{max}$ (see Fig. 7) and g_{max} (see Fig. 10) as obtained from single-channel and whole-cell experiments, respectively, we conclude that the observed pH_o-induced modulation of current amplitude is due to (*a*) changes in the single-channel conductance as well as in the probability of the T-type Ca channel being open, and (*b*) the titration of the negative surface charges in the neighborhood of the T-type channel as measured in the whole-cell experiments.

The absence of pH_o-induced gating shifts in the single-channel experiments in contrast to the whole-cell experiments might explain the discrepancy between the pH_o-induced changes in time constants of activation of the currents as observed in the whole-cell mode and not in the single-channel experiments. In accord with these findings, kinetic parameters (τ_{c1}, τ_{c2}, τ_o, t_L, t_o, and t_{cl}) did not vary for changes in pH_o

between pH 6 and 9 in our single-channel experiments. It must, however, be mentioned that with the small and fast events of the T-type channel, the kinetic analysis stressed above could be contaminated by false positive events (overlap of Gaussians at the midpoint between open and closed levels), as well as by missed short events.

Proton modulation of the T-type Ca channel acts from outside. In contrast to the L-type channel, we conclude that changes in the internal proton concentration (pH range 6–9) do not modulate T-type currents and hence, that the proton modulation of the T-type Ca channel acts from outside. In our single-channel experiments, a change in the extracellular pH (i.e., in the pipette) induces changes in the single-channel conductance and in the occurrence of blank and nonblank sweeps. Since these experiments are performed in the cell-attached mode, it is very unlikely that the different proton concentrations of the pipette solution have influenced the pH of the cell interior. Other evidence for the external proton modulation is based on our whole-cell experiments in which the current densities are identical whatever the pH of the pipette solution is: 6.5, 7.2, or 8. Moreover, raising the internal HEPES concentration from 10 to 50 mM does not change the extent of pH_o-modulated Ca channel currents. The effects of a change in external pH also are always rapid. In contrast, a rapid change in the internal pH would require an appreciable current of protons, and such an H^+ inward current would depolarize the resting membrane. Possible secondary pH_i-mediated effects via the Na-H exchange system are excluded in our experiments by superfusing the cells with a Na-deficient solution (Tris substituted) that blocks this exchange mechanism.

For the L-type Ca channel, Krafte and Kass (1988) have shown that a threefold increase of the internal HEPES concentration from 10 to 30 mM gives comparable effects on the L-type Ca current for given changes in pH_o. From their experiments they concluded that secondary changes in pH_i after a change in pH_o seem absent. In contrast, in the work of Irisawa and Sato (1986), pH_i effects on the L-type Ca channel do exist and are very dependent on the Na-H exchange system. Furthermore, they reported that an intracellular pH of 6.5 reduces the L-type Ca current by 50%. This suppressive effect of intracellular acidification on the L-type Ca current, as observed in whole-cell experiments, is further supported on the single-channel level by Kaibara and Kameyama (1988). These authors concluded that the single-channel conductance of the L-type Ca channel was decreased upon lowering the internal pH. They also showed that the percentage of blank sweeps was increased upon lowering pH_i, while that of nonblank sweeps was decreased.

In summary, we conclude that the proton modulation of the T-type Ca channel observed in our experiments acts from outside. In this respect, the proton modulation of the L-type Ca channel, as described in the literature, seems to occur differently.

Physiological Relevance

The physiological role of the T-type Ca channel in cardiac tissue remains poorly understood. Because of its negative range of activation, the channel might be involved in pacemaker activity in cardiac cells as proposed by Bean (1985) and Nilius et al. (1985), and demonstrated by Nilius (1986). Recently, Hagiwara et al. (1988)

have shown that T-type Ca channels participate in the latter half of the diastolic depolarization in sino-atrial node cells. Since a slight reduction or increase of pH_o affects the T-type Ca channel quite heavily, it seems possible that the pH-induced effects on the T-type Ca channel play a role in changes of diastolic depolarization of nodal action potentials of the rabbit (Satoh and Seyama, 1986).

We thank Mr. J. Prenen for his help during the experiments, Dr. J. Vereecke for critical comments, Mrs. L. Heremans for preparing the solutions, and Mr. M. Coenen for the photography. We gratefully acknowledge Dr. G. Droogmans' help in providing us with computer programs for single-channel data analysis.

Bernd Nilius was supported by grants from the KU Leuven and the Ministry of Public Health. Jan Tytgat was supported by the National Fund for Scientific Research (Belgium), of which he is a Research Assistant.

Original version received 3 January 1990 and accepted version received 16 April 1990.

REFERENCES

Bean, B. P. 1985. Two kinds of calcium channels in canine atrial cells. *Journal of General Physiology.* 86:1–30.

Begenisich, T., and M. Danko. 1983. Hydrogen ion block of the sodium pore in squid giant axons. *Journal of General Physiology.* 82:599–618.

Bevington, P. R. 1969. Data Reduction and Error Analysis for the Physical Sciences. McGraw-Hill Inc., New York.

Bonvallet, R. 1987. A low threshold calcium current recorded at physiological Ca concentrations in single frog atrial cells. *Pflügers Archiv.* 408:540–542.

Carbone, E., and H. D. Lux. 1984. A low voltage-activated, fully inactivating Ca channel in vertebrate sensory neurones. *Nature.* 310:501–502.

Carbone, E., and H. D. Lux. 1987*a*. Kinetics and selectivity of a low-voltage-activated calcium current in chick and rat sensory neurones. *Journal of Physiology.* 386:547–570.

Carbone, E., and H. D. Lux. 1987*b*. Single low-voltage-activated calcium channels in chick and rat sensory neurones. *Journal of Physiology.* 386:571–601.

Chesnais, J. M., E. Coraboeuf, M. P. Sauviat, and J. M. Vassas. 1975. Sensitivity to H, Li and Mg ions of slow inward sodium current in frog atrial fibres. *Journal of Molecular and Cellular Cardiology.* 7:627–642.

Droogmans, G., and B. Nilius. 1989. Kinetic properties of the cardiac T-type calcium channel in the guinea-pig. *Journal of Physiology.* 419:627–650.

Fox, A. P., M. C. Nowycky, and R. W. Tsien. 1987*a*. Kinetic and pharmacological properties distinguishing three types of calcium currents in chick sensory neurones. *Journal of Physiology.* 394:149–172.

Fox, A. P., M. C. Nowycky, and R. W. Tsien. 1987*b*. Single-channel recordings of three types of calcium channels in chick sensory neurones. *Journal of Physiology.* 394:173–200.

Hagiwara, N., H. Irisawa, and M. Kameyama. 1988. Contribution of two types of calcium currents to the pacemaker potentials of rabbit sino-atrial node cells. *Journal of Physiology.* 395:233–253.

Hamill, O. P., A. Marty, E. Neher, B. Sakmann, and F. J. Sigworth. 1981. Improved patch-clamp techniques for high-resolution current recording from cells and cell-free membrane patches. *Pflügers Archiv.* 391:85–100.

Hess, P. 1988. Elementary properties of cardiac calcium channels: a brief review. *Canadian Journal of Physiology and Pharmacology.* 66:1218–1223.

Iijima, T., S. Ciani, and S. Hagiwara. 1986. Effects of the external pH on Ca channels: experimental studies and theoretical considerations using a two-site, two-ion model. *Proceedings of the National Academy of Sciences USA.* 83:654–658.

Irisawa, H., and R. Sato. 1986. Intra- and extracellular actions of proton on the calcium current of isolated guinea pig ventricular cells. *Circulation Research.* 59:348–355.

Kaibara, M., and M. Kameyama. 1988. Inhibition of the calcium channel by intracellular protons in single ventricular myocytes of the guinea-pig. *Journal of Physiology.* 403:621–640.

Krafte, D. S., and R. S. Kass. 1988. Hydrogen ion modulation of Ca channel current in cardiac ventricular cells. *Journal of General Physiology.* 91:641–657.

Kurachi, Y. 1982. The effects of intracellular protons on the electrical activity of single ventricular cells. *Pflügers Archiv.* 394:264–270.

Mitra, R., and M. Morad. 1985. A uniform enzymatic method for dissociation of myocytes from hearts and stomachs of vertebrates. *American Journal of Physiology.* 249:H1056–H1060.

Mitra, R., and M. Morad. 1986. Two types of calcium channels in guinea pig ventricular myocytes. *Proceedings of the National Academy of Sciences USA.* 83:5340–5344.

Nilius, B. 1986. Possible functional significance of a novel type of cardiac Ca channel. *Biomedica Biochimica Acta.* 45:K37–K45.

Nilius, B., P. Hess, J. B. Lansman, and R. W. Tsien. 1985. A novel type of cardiac calcium channel in ventricular cells. *Nature.* 316:443–446.

Ohmori, H., and M. Yoshii. 1977. Surface potential reflected in both gating and permeation mechanisms of sodium and calcium channels of the tunicate egg cell membrane. *Journal of Physiology.* 267:429–463.

Pietrobon, D., B. Prod'hom, and P. Hess. 1988. Conformational changes associated with ion permeation in L-type calcium channels. *Nature.* 333:373–376.

Prod'hom, B., D. Pietrobon, and P. Hess. 1987. Direct measurement of proton transfer rates to a group controlling the dihydropyridine-sensitive Ca^{2+} channel. *Nature.* 329:243–246.

Sato, R., A. Noma, Y. Kurachi, and H. Irisawa. 1985. Effects of intracellular acidification on membrane currents in ventricular cells of the guinea pig. *Circulation Research.* 57:553–561.

Satoh, H., and I. Seyama. 1986. On the mechanism by which changes in extracellular pH affect the electrical activity of the rabbit sino-atrial node. *Journal of Physiology.* 381:181–191.

Tytgat, J., B. Nilius, J. Vereecke, and E. Carmeliet. 1988*a*. The T-type Ca channel in guinea-pig ventricular myocytes is insensitive to isoproterenol. *Pflügers Archiv.* 411:704–706.

Tytgat, J., J. Vereecke, and E. Carmeliet. 1988*b*. Differential effects of verapamil and flunarizine on cardiac L-type and T-type Ca channels. *Naunyn-Schmiedeberg's Archives of Pharmacology.* 337:690–692.

Yatani, A., and M. Goto. 1983. The effect of extracellular low pH on the plateau current in isolated, single rat ventricular cells: a voltage clamp study *Japanese Journal of Physiology.* 33:403–415.